A&A 602, C2 (2017)
DOI: 10.1051/0004-6361/201525666e

Astronomy & Astrophysics

The catalogue of radial velocity variable hot subluminous stars from the MUCHFUSS project *(Corrigendum)*

S. Geier[1,2], T. Kupfer[3], U. Heber[2], V. Schaffenroth[2,4], B. N. Barlow[5], R. H. Østensen[6], S. J. O'Toole[7], E. Ziegerer[2], C. Heuser[2], P. F. L. Maxted[8], B. T. Gänsicke[9], T. R. Marsh[9], R. Napiwotzki[10], P. Brünner[2], M. Schindewolf[2], and F. Niederhofer[1]

[1] European Southern Observatory, Karl-Schwarzschild-Str. 2, 85748 Garching, Germany
e-mail: sgeier@eso.org
[2] Dr. Karl Remeis-Observatory & ECAP, Astronomical Institute, Friedrich-Alexander University Erlangen-Nuremberg, Sternwartstr. 7, 96049 Bamberg, Germany
[3] Department of Astrophysics/IMAPP, Radboud University Nijmegen, PO Box 9010, 6500 GL Nijmegen, The Netherlands
[4] Institute for Astro- and Particle Physics, University of Innsbruck, Technikerstr. 25/8, 6020 Innsbruck, Austria
[5] Department of Physics, High Point University, One University Parkway, High Point, NC 27268, USA
[6] Institute of Astronomy, KU Leuven, Celestijnenlaan 200D, 3001 Heverlee, Belgium
[7] Australian Astronomical Observatory, PO Box 915, North Ryde NSW 1670, Australia
[8] Astrophysics Group, Keele University, Staffordshire, ST5 5BG, UK
[9] Department of Physics, University of Warwick, Conventry CV4 7AL, UK
[10] Centre of Astrophysics Research, University of Hertfordshire, College Lane, Hatfield AL10 9AB, UK

A&A 577, A26 (2015), DOI: 10.1051/0004-6361/201525666

Key words. binaries: spectroscopic – subdwarfs – stars: horizontal branch – stars: atmospheres – errata, addenda

The function we used to calculate the logarithm of the false-detection probability provides the natural logarithm $\ln p$ and not the decadal logarithm as incorrectly assumed in the paper. This mildy affects the number of radial velocity (RV) variable stars and significantly the number of RV variable candidates in our sample. The conclusions of the paper essentially remain the same.

We consider the detection of RV variability to be significant, if the false-detection probability p is smaller than 0.01% ($\ln p < -9.2$). The fraction of such significant detections in our initial sample of 196 is now 39% (76 objects). Objects with false-detection probabilities between 0.01% and 5% ($\ln p = -9.2$ to $\ln p = -3.0$) are regarded as candidates for RV variability and constitute 27% of the initial sample (53 objects). About 34% ($\ln p > -3.0$, 67 objects) are regarded as non-detections. Removing those non-detections we end up with a sample of 129 stars, which show RV variability with probabilites between 95% and 99.9% (see Table 1).

Tables 3–5 and A.1 as well as Figures 1–6 of the original paper have been updated (Tables 2–5, Figs. 1–4).

The corrected upper limit for the fraction of extremely close binary sdB+NS/BH binaries is 1.5% instead of 1.3%.

The RV-variable sample now contains 18 helium-rich hot subdwarf stars. 6 of them show significant RV variations while 12 qualify as candidates (see Table 3). The He-sdOB J160450.44+051909.2 discussed in the paper is not regarded as RV-variable candidate any more.

Table 1. Sample statistics.

Class	RV variable	RV variable candidates	Non-detections
H-rich sdO/B	65	36	51
He-rich sdO/B	6	12	11
Others	5	5	5
Total	76	53	67

References

Althaus, L. G., Panei, J. A., Miller Bertolami, M. M., et al. 2009, ApJ, 704, 1605
Dorman, B., Rood, R. T., & O'Connell, R. W. 1993, ApJ, 419, 596
Driebe, T., Schönberner, D., Bloecker, T., & Herwig, F. 1998, A&A, 339, 123
Geier, S., Hirsch, H., Tillich, A., et al. 2011a, A&A, 530, A28
Geier, S., Maxted, P. F. L., Napiwotzki, R., et al. 2011b, A&A, 526, A39
Geier, S., Schaffenroth, V., Drechsel, H., et al. 2011c, ApJ, 731, L22
Kupfer, T., Geier, S., Schaffenroth, V., et al. 2015, A&A, 576, A44
Østensen, R. H., Geier, S., Schaffenroth, V., et al. 2013, A&A, 559, A35
Schaffenroth, V., Geier, S., Heber, U., et al. 2014, A&A, 564, A98
Reindl, N., Geier, S., Kupfer, T., et al. 2016, A&A, 587, A101
Schaller, G., Schaerer, D., Meynet, G., & Maeder, A. 1992, A&AS, 96, 269
Schönberner, D. 1983, ApJ, 272, 708
Werner, K., Rauch, T., & Kepler, S. O. 2014, A&A, 564, A53

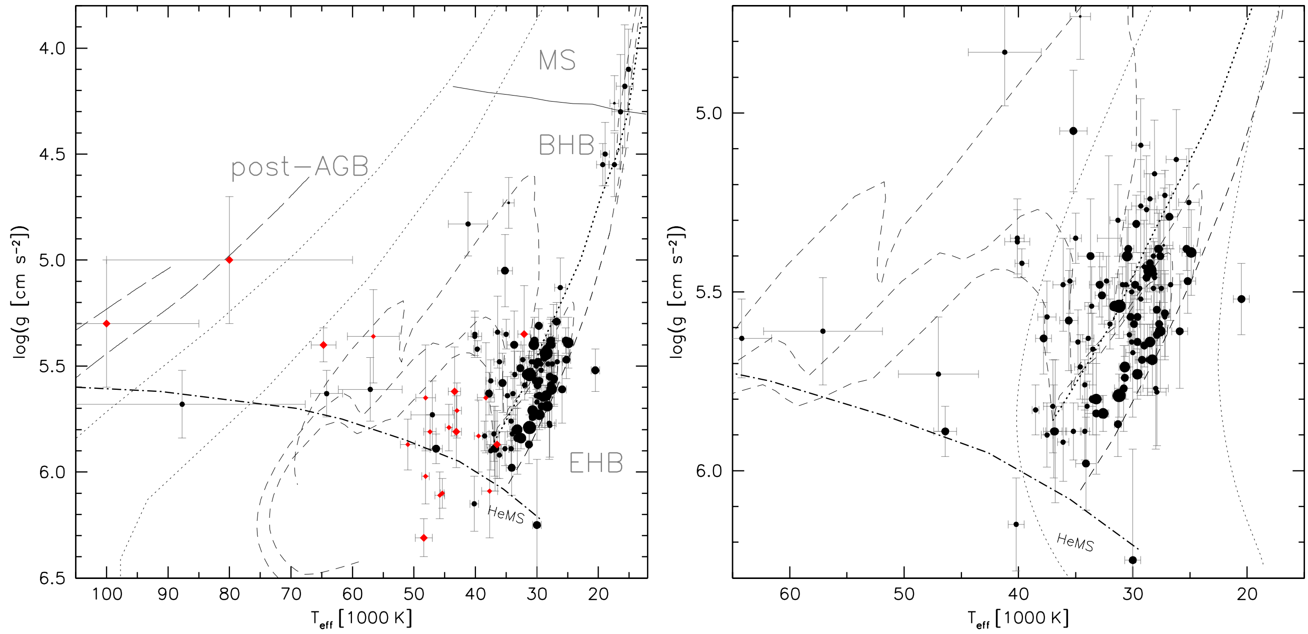

Fig. 1. *Left panel*: $T_{\rm eff} - \log g$ diagram of the full sample of hot, subluminous, RV-variable stars. The size of the symbols scales with $\Delta RV_{\rm max}$. The black circles mark stars with hydrogen dominated atmospheres ($\log y < 0$), while the red diamonds mark stars with helium dominated atmospheres. The helium main sequence (HeMS) and the HB band are superimposed with HB evolutionary tracks (dashed lines) for subsolar metallicity ($\log z = -1.48$) from Dorman et al. (1993). The three tracks in the high temperature range correspond to helium core masses of 0.488, 0.490 and 0.495 $M_\odot$ (from bottom-left to top-right). Those tracks mark the EHB evolution, since the stars do not reascend the giant branch in the helium shell-burning phase. The two tracks in the upper right correspond to core masses of 0.53 and 0.54 $M_\odot$. Blue horizontal branch stars following those tracks are expected to experience a second giant phase. The solid line marks the relevant part of the zero-age main sequence for solar metallicity taken from Schaller et al. (1992). The two dotted lines are post-AGB tracks for hydrogen-rich stars with masses of 0.546 (lower line) and 0.565 $M_\odot$ (upper line) taken from Schönberner (1983). The two long-dashed lines are post-AGB tracks for helium-rich stars with masses of 0.53 (lower line) and 0.609 $M_\odot$ (upper line) taken from Althaus et al. (2009). *Right panel*: $T_{\rm eff} - \log g$ diagram of RV variable hydrogen-rich sdB and sdOB stars. The two dotted lines mark post-RGB tracks (Driebe et al. 1998) for core masses of 0.234 (left) and 0, 259 $M_\odot$ (right).

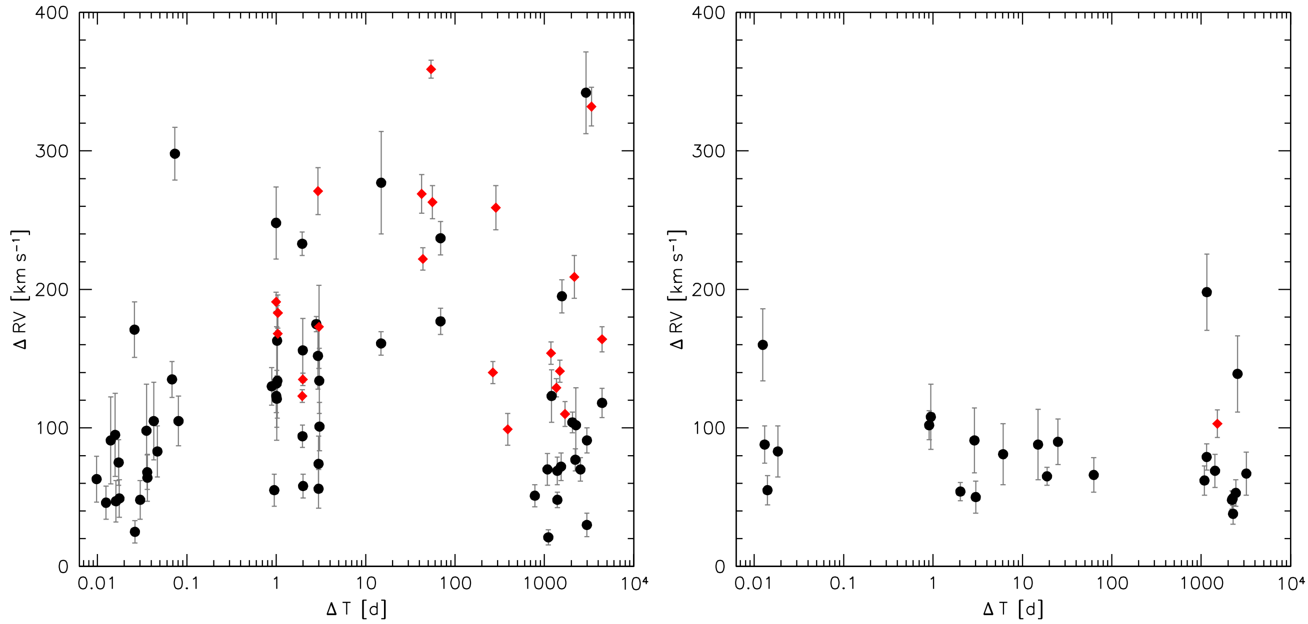

Fig. 2. *Left panel*: highest RV shift between individual spectra plotted against time difference between the corresponding observing epochs. The filled red diamonds mark sdB binaries with known orbital parameters (Kupfer et al. 2015), while the filled black circles mark the rest of the hydrogen-rich sdB sample of RV variable stars. *Right panel*: the same plot for the hydrogen-rich sdOB and sdO sample of RV variable stars.

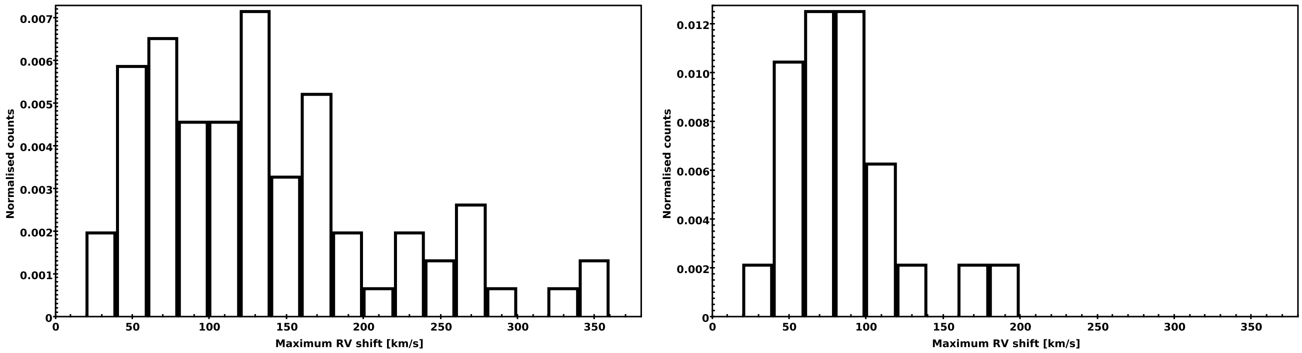

Fig. 3. ΔRV_{max} distribution of RV-variable sdB stars (*left panel*) as well as sdOB and sdO stars with hydrogen-rich atmospheres (*right panel*).

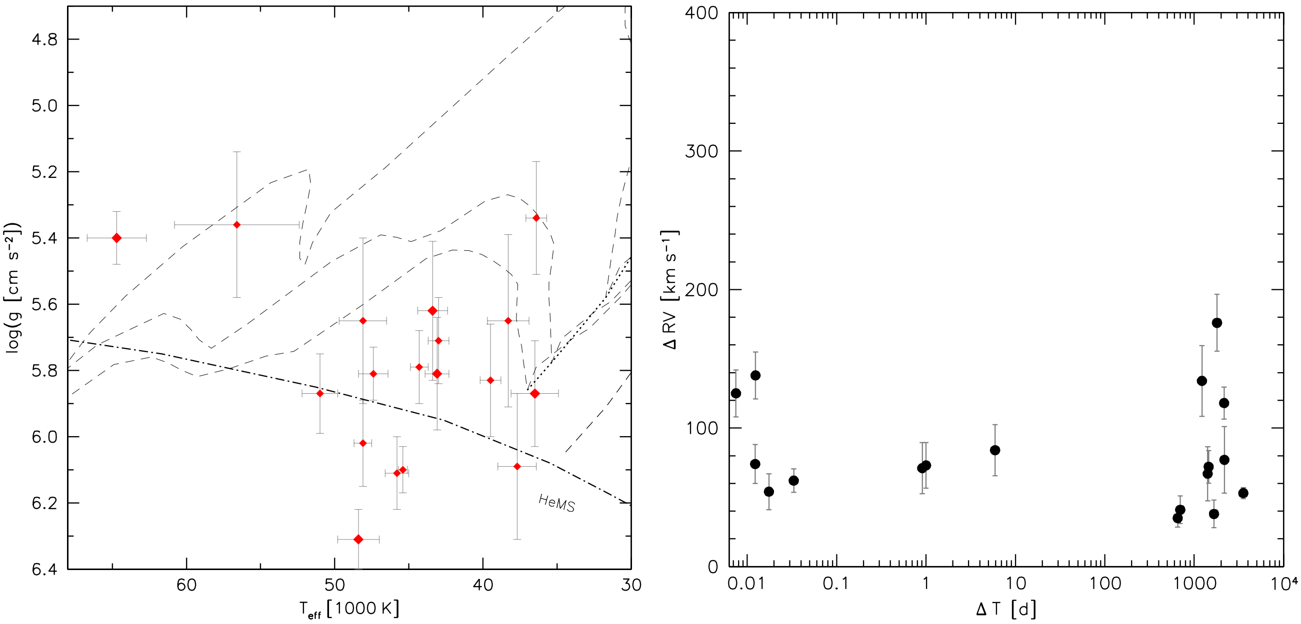

Fig. 4. *Left panel*: $T_{\rm eff} - \log g$ diagram of RV variable helium-rich sdOB and sdO stars (see Fig. 1). The size of the symbols scales with ΔRV_{max}. The helium main sequence (HeMS) and the HB band are superimposed with HB evolutionary tracks (dashed lines) for subsolar metallicity ($\log z = -1.48$) from Dorman et al. (1993). The three tracks correspond to helium core masses of 0.488, 0.490 and 0.495 $M_{\odot}$ (from bottom-left to top-right). *Right panel*: highest RV shift between individual spectra plotted against time difference between the corresponding observing epochs for helium-rich sdO and sdOB stars (see Fig. 2).

Table 2. Parameters of 101 hydrogen-rich hot subdwarfs (65 RV variable, 36 RV variable candidates).

Name	Class	m_V [mag]	$T_{\rm eff}$ [K]	$\log g$	$\log y$	d [kpc]	Δt [d]	$\Delta RV_{\rm max}$ [km s^{-1}]	N	$\ln p$
J082332.09+113641.9[b]	sdB	16.7	31 200 ± 600	5.79 ± 0.06	−2.0 ± 0.1	$2.6^{+0.2}_{-0.2}$	53.9447	359.0 ± 6.5	22	<−680
J113840.68-003531.7[c]	sdB	14.5	31 200 ± 600	5.54 ± 0.09	<−3.0	$1.2^{+0.2}_{-0.1}$	3361.5592	332.0 ± 14.0	31	<−680
J165404.26+303701.8[c]	sdB	15.4	24 900 ± 800	5.39 ± 0.12	−2.4 ± 0.1	$1.8^{+0.3}_{-0.3}$	2.9365	271.0 ± 17.0	38	<−680
J225638.34+065651.1[c]	sdB	15.3	28 500 ± 500	5.64 ± 0.05	−2.3 ± 0.2	$1.5^{+0.1}_{-0.1}$	42.3494	269.0 ± 14.0	50	<−680
J172624.10+274419.3[c]	sdB	16.0	32 600 ± 500	5.84 ± 0.05	−2.2 ± 0.1	$1.9^{+0.1}_{-0.1}$	55.9741	263.0 ± 12.0	38	<−680
J150513.52+110836.6[c]	sdB	15.4	33 200 ± 500	5.80 ± 0.10	−2.3 ± 0.1	$1.5^{+0.2}_{-0.2}$	43.6564	222.0 ± 8.0	42	<−680
J134632.66+281722.7[b]	sdB	14.9	28 800 ± 600	5.46 ± 0.07	−2.6 ± 0.2	$1.6^{+0.2}_{-0.1}$	0.9988	191.0 ± 7.0	41	<−680
J002323.99-002953.2[c]	sdB	15.5	29 200 ± 500	5.69 ± 0.05	−2.0 ± 0.1	$1.6^{+0.1}_{-0.1}$	1.0413	168.0 ± 4.0	47	<−680
J083006.17+475150.4[b]	sdB	16.0	25 300 ± 600	5.38 ± 0.06	<−3.0	$2.5^{+0.2}_{-0.2}$	4405.6747	164.0 ± 9.0	37	<−680
J095238.93+625818.9[b]	sdB	14.8	27 700 ± 600	5.59 ± 0.06	−2.6 ± 0.1	$1.2^{+0.1}_{-0.1}$	1183.7390	154.0 ± 8.0	34	<−680
J162256.66+473051.1[d]	sdB	16.2	29 000 ± 600	5.65 ± 0.06	−1.9 ± 0.1	$2.3^{+0.2}_{-0.2}$	1.9832	135.0 ± 4.5	34	<−680
J012022.94+395059.4[e]	sdB	15.4	28 500 ± 100	5.42 ± 0.01	−3.0 ± 0.1	$2.1^{+0.0}_{-0.0}$	1358.9782	129.0 ± 6.5	22	<−680
J173606.25+315842.7	sdB	17.0	31 300 ± 300	5.87 ± 0.09	−2.5 ± 0.2	$2.8^{+0.3}_{-0.3}$	1567.7104	195.0 ± 12.0	12	−537.49
J032138.67+053840.0[b]	sdB	15.0	30 700 ± 500	5.74 ± 0.06	−2.4 ± 0.1	$1.3^{+0.1}_{-0.1}$	1699.1435	110.0 ± 9.0	46	−536.46
J191908.76+371423.9	sdB	17.2	28 300 ± 400	5.69 ± 0.10	−2.7 ± 0.3	$3.4^{+0.5}_{-0.4}$	68.8608	237.0 ± 12.0	15	−526.21
J102151.64+301011.9[a]	sdB	18.3	30 700 ± 500	5.71 ± 0.06	<−3.0	$5.8^{+0.5}_{-0.5}$	14.9363	277.0 ± 37.0	19	−508.16
J204613.40-045418.7[c]	sdB	16.2	31 600 ± 500	5.54 ± 0.08	<−3.0	$2.8^{+0.3}_{-0.3}$	286.2265	259.0 ± 16.0	22	−480.28
J173806.51+451701.7	sdB	17.4	30 500 ± 500	5.40 ± 0.08	<−3.0	$5.5^{+0.6}_{-0.6}$	1.9536	233.0 ± 8.5	13	−461.58
J183249.04+630910.7[b]	sdB	15.8	26 800 ± 700	5.29 ± 0.09	−2.6 ± 0.1	$2.7^{+0.4}_{-0.3}$	1487.7733	141.0 ± 8.0	17	−453.62
J164326.04+330113.1[a]	sdB	16.3	27 900 ± 500	5.62 ± 0.07	−2.3 ± 0.2	$2.4^{+0.2}_{-0.2}$	2.8085	175.0 ± 5.5	10	−452.26
J011857.19-002546.5[b]	sdB	14.9	27 900 ± 600	5.55 ± 0.07	<−3.0	$1.3^{+0.1}_{-0.1}$	265.2187	140.0 ± 8.0	43	−386.44
J192059.78+372220.0[f]	sdB	15.8	27 600 ± 600	5.40 ± 0.10	−2.5 ± 0.3	$2.4^{+0.3}_{-0.3}$	1.9589	123.0 ± 4.5	15	−319.72
J150829.02+494050.9[b]	sdB	17.7	29 600 ± 600	5.73 ± 0.07	−2.3 ± 0.1	$4.3^{+0.5}_{-0.4}$	2161.9292	209.0 ± 15.5	58	−269.10
J180940.41+234328.4	sdB	16.5	28 500 ± 300	5.44 ± 0.06	−2.9 ± 0.2	$3.3^{+0.3}_{-0.3}$	2909.9029	342.0 ± 29.5	36	−215.11
J183349.79+652056.3	sdB	17.4	27 200 ± 500	5.56 ± 0.12	−2.6 ± 0.1	$4.1^{+0.7}_{-0.6}$	68.8591	177.0 ± 9.5	16	−190.20
J095101.28+034757.0[b]	sdB	15.9	29 800 ± 300	5.48 ± 0.04	−2.8 ± 0.3	$2.5^{+0.1}_{-0.1}$	1.0425	183.0 ± 13.0	31	−170.79
J082053.53+000843.4[g]	sdB	15.2	26 700 ± 900	5.48 ± 0.10	−2.0 ± 0.1	$1.6^{+0.3}_{-0.2}$	388.9794	99.0 ± 11.5	24	−153.08
J080738.96-083322.6	sdB	17.2	27 600 ± 600	5.61 ± 0.17	−2.7 ± 0.3	$3.6^{+0.9}_{-0.7}$	0.0736	298.0 ± 19.0	27	−136.25
J152222.15-013018.3[b]	sdB	17.8	25 200 ± 700	5.47 ± 0.09	<−3.0	$5.2^{+0.7}_{-0.6}$	3.0055	173.0 ± 30.0	26	−126.07
J155628.34+011335.0[a]	sdB	16.2	32 700 ± 600	5.51 ± 0.08	−2.9 ± 0.2	$3.1^{+0.4}_{-0.3}$	4412.8910	118.0 ± 10.5	15	−121.64
J113241.58-063652.8[b]	sdO	16.2	46 400 ± 1000	5.89 ± 0.07	−2.9 ± 0.2	$2.4^{+0.2}_{-0.2}$	1517.8240	103.0 ± 10.0	32	−108.89
J222850.00+391917.4	sdB	16.4	33 500 ± 900	5.80 ± 0.10	−1.7 ± 0.1	$2.4^{+0.4}_{-0.3}$	2051.8410	104.0 ± 7.5	40	−85.63
J173057.94+320737.0	sdB	16.2	28 200 ± 700	5.40 ± 0.05	−2.9 ± 0.2	$3.0^{+0.2}_{-0.2}$	1.9680	94.0 ± 8.0	6	−69.42
J083334.76-045759.4	sdB	18.2	20 500 ± 700	5.52 ± 0.10	<−3.0	$5.0^{+0.8}_{-0.7}$	14.8908	161.0 ± 8.5	11	−66.11
J164853.26+121703.0	sdB	18.5	30 400 ± 500	5.38 ± 0.11	<−3.0	$9.3^{+1.4}_{-1.2}$	0.0684	135.0 ± 13.0	11	−64.89
J072245.27+305233.4	sdB	18.0	25 900 ± 700	5.61 ± 0.16	−2.6 ± 0.2	$5.0^{+1.2}_{-0.9}$	1.0019	123.0 ± 12.0	7	−62.09
J093059.63+025032.3	sdB	15.0	30 000 ± 600	5.67 ± 0.18	−2.7 ± 0.2	$1.3^{+0.3}_{-0.3}$	2986.7695	91.0 ± 9.0	10	−49.22
J203526.46+141948.4	sdB	18.7	30 200 ± 600	5.57 ± 0.07	−2.9 ± 0.2	$8.3^{+0.9}_{-0.8}$	1.0235	163.0 ± 25.5	12	−33.12
J203843.97+141706.0	sdOB	18.7	36 800 ± 1000	5.89 ± 0.20	−2.4 ± 0.3	$6.8^{+1.9}_{-1.5}$	0.9067	102.0 ± 10.5	12	−32.22
J095229.62+301553.6[a]	sdOB	18.5	35 200 ± 1200	5.05 ± 0.17	<−3.0	$16.0^{+3.8}_{-3.3}$	1155.7612	198.0 ± 27.5	5	−28.52
J154531.01+563944.7	sdB	17.0	26 200 ± 900	5.13 ± 0.14	−2.0 ± 0.2	$5.5^{+1.2}_{-1.0}$	2527.7769	70.0 ± 8.5	9	−27.76
J200959.27-115519.9	sdB	18.7	29 700 ± 700	5.31 ± 0.08	<−3.0	$10.7^{+1.3}_{-1.2}$	1.9832	156.0 ± 23.0	8	−27.48
J005107.01+004232.5	sdOB	15.9	38 500 ± 300	5.83 ± 0.07	−1.0 ± 0.1	$2.0^{+0.2}_{-0.2}$	2.0256	54.0 ± 6.5	7	−24.96
J104248.94+033355.3	sdO	17.6	41 200 ± 3200	4.83 ± 0.15	−2.1 ± 0.4	$14.5^{+3.4}_{-2.8}$	2246.6948	49.0 ± 5.0	2	−24.34
J181141.86+241902.7	sdB	18.7	–	–	–	–	0.9972	248.0 ± 26.0	7	−23.56
J071424.12+401645.9	sdB	18.2	27 700 ± 700	5.38 ± 0.11	−2.6 ± 0.1	$7.6^{+1.2}_{-1.1}$	2.9312	152.0 ± 24.0	9	−23.37
J204300.90+002145.0[a]	sdO	17.9	40 200 ± 700	6.15 ± 0.13	−1.3 ± 0.4	$3.6^{+0.6}_{-0.5}$	18.8480	65.0 ± 6.5	9	−22.54
J191645.87+371224.5	sdB	18.3	33 200 ± 1000	5.84 ± 0.17	−2.7 ± 0.2	$5.6^{+1.4}_{-1.1}$	3.0338	134.0 ± 23.5	19	−22.15
J094750.71+162731.8	sdB	17.4	30 000 ± 700	6.25 ± 0.31	−2.2 ± 0.3	$2.1^{+1.0}_{-0.7}$	0.8902	130.0 ± 13.5	5	−20.08
J115358.81+353929.0[a]	sdOB	16.6	29 400 ± 500	5.49 ± 0.06	−2.5 ± 0.3	$3.3^{+0.3}_{-0.3}$	1151.6544	79.0 ± 9.5	5	−19.15
J175125.67+255003.5[a]	sdB	17.4	30 600 ± 500	5.48 ± 0.08	<−3.8	$5.0^{+0.6}_{-0.5}$	1533.6229	72.0 ± 10.0	8	−16.50
J125702.30+435245.8[a]	sdB	18.2	28 000 ± 1100	5.77 ± 0.17	<−3.0	$4.9^{+1.3}_{-1.0}$	0.0098	63.0 ± 16.5	3	−16.32
J165446.26+182224.6	sdB	18.6	30 100 ± 500	5.50 ± 0.08	−1.7 ± 0.1	$8.5^{+1.0}_{-0.9}$	1396.0335	48.0 ± 5.5	3	−15.27
J120855.51+403716.1	sdB	18.6	34 100 ± 900	5.98 ± 0.13	−1.5 ± 0.1	$5.4^{+1.0}_{-0.9}$	0.0260	171.0 ± 20.0	7	−14.61
J164122.32+334452.0	sdB	15.5	28 200 ± 500	5.49 ± 0.11	−2.5 ± 0.3	$1.9^{+0.3}_{-0.3}$	2213.5393	77.0 ± 8.0	8	−14.60
J211421.39+100411.4	sdOB	18.4	36 100 ± 900	5.48 ± 0.13	−2.5 ± 0.3	$9.2^{+1.6}_{-1.4}$	1427.1132	69.0 ± 12.0	7	−14.02
J170810.97+244341.6[a]	sdOB	18.5	35 600 ± 800	5.58 ± 0.14	−0.8 ± 0.1	$8.5^{+1.6}_{-1.4}$	0.0125	160.0 ± 26.0	3	−13.73
J153411.10+543345.2[a]	sdOB	16.9	34 800 ± 700	5.64 ± 0.09	−2.6 ± 0.3	$3.8^{+0.5}_{-0.4}$	0.0184	83.0 ± 18.5	8	−12.52
J224518.65+220746.5	sdB	16.6	34 000 ± 800	5.82 ± 0.07	−2.2 ± 0.1	$2.6^{+0.3}_{-0.3}$	1080.8857	70.0 ± 11.5	9	−12.28
J120613.40+205523.1	sdOB	18.4	35 000 ± 500	5.35 ± 0.07	<−3.0	$10.5^{+1.0}_{-0.9}$	2.9112	91.0 ± 23.5	10	−11.37
J204247.51+001913.9[h]	sdB	19.6	34 200 ± 400	5.89 ± 0.08	−1.3 ± 0.1	$9.6^{+1.1}_{-1.0}$	1393.1941	69.0 ± 10.0	3	−10.83
J151314.23+234248.8	sdB	17.1	28 700 ± 300	5.69 ± 0.10	−2.3 ± 0.2	$3.3^{+0.4}_{-0.4}$	2.0006	58.0 ± 8.5	3	−10.83
J082944.75+132302.5	sdOB	17.2	39 700 ± 600	5.42 ± 0.04	<−3.0	$6.1^{+0.3}_{-0.3}$	24.9992	90.0 ± 16.5	5	−10.40

Notes. Solved binaries are marked in bold face and their orbital parameters can be found in Kupfer et al. (2015) and references therein. [(a)] Atmospheric parameters taken from Geier et al. (2011a). [(b)] Atmospheric parameters taken from Kupfer et al. (2015). [(c)] Atmospheric parameters taken from Geier et al. (2011b). [(d)] Atmospheric parameters taken from Schaffenroth et al. (2014). [(e)] Atmospheric parameters taken from Østensen et al. (2013). [(f)] Atmospheric parameters taken from Schaffenroth et al. (in prep.). [(g)] Atmospheric parameters taken from Geier et al. (2011c). [(h)] Atmospheric parameters derived from a spectrum taken with ESO-VLT/FORS1. [(i)] Atmospheric parameters derived from a spectrum taken with WHT/ISIS.

Table 2. continued.

Name	Class	m_V [mag]	$T_{\rm eff}$ [K]	$\log g$	$\log y$	d [kpc]	Δt [d]	$\Delta RV_{\rm max}$ [km s^{-1}]	N	$\ln p$
J074534.16+372718.5[a]	sdB	17.9	37 500 ± 500	5.90 ± 0.09	<−3.0	$4.6^{+0.5}_{-0.5}$	0.0363	64.0 ± 17.0	8	−9.74
J202313.83+131254.9[a]	sdB	17.2	29 600 ± 600	5.64 ± 0.14	−2.1 ± 0.1	$3.8^{+0.7}_{-0.6}$	1201.7981	123.0 ± 19.0	5	−9.20
J162610.34+130401.6	sdB	19.4	33 900 ± 500	5.63 ± 0.10	−1.0 ± 0.1	$12.1^{+1.7}_{-1.5}$	780.7541	51.0 ± 8.0	3	*−9.16*
J030607.95+382335.7[i]	sdO	16.8	30 100 ± 300	5.64 ± 0.03	−2.1 ± 0.1	$3.2^{+0.1}_{-0.1}$	2210.7452	48.0 ± 6.5	8	*−8.85*
J204451.08-062753.8	sdO	20.0	57 100 ± 5200	5.61 ± 0.15	−2.2 ± 0.4	$21.4^{+5.1}_{-4.2}$	1087.0571	62.0 ± 10.5	3	*−7.88*
J091615.49+132833.1	sdB	17.5	30 900 ± 400	5.48 ± 0.05	<−3.0	$5.4^{+0.4}_{-0.4}$	0.9512	55.0 ± 11.5	3	*−7.58*
J163413.09+163109.5	sdB	18.3	34 600 ± 900	4.73 ± 0.12	−2.0 ± 0.5	$20.7^{+3.5}_{-3.1}$	1105.3751	21.0 ± 5.5	3	*−7.44*
J123220.09+260913.3	sdB	18.1	33 700 ± 1100	5.40 ± 0.16	−1.3 ± 0.2	$8.5^{+2.0}_{-1.7}$	1.0302	134.0 ± 27.0	5	*−7.36*
J185129.02+182358.8	sdB	16.8	27 800 ± 700	5.38 ± 0.10	<−3.0	$3.9^{+0.6}_{-0.5}$	0.0808	105.0 ± 18.0	22	*−7.33*
J220048.67+123612.4[h]	sdO	18.6	64 200 ± 2600	5.63 ± 0.11	−1.3 ± 0.1	$11.4^{+1.8}_{-1.6}$	2437.2535	53.0 ± 9.5	3	*−7.04*
J153752.95+160201.8	sdB	18.4	32 300 ± 500	5.47 ± 0.07	<−3.0	$8.5^{+0.9}_{-0.8}$	0.0361	68.0 ± 12.5	3	*−7.03*
J183229.22+402418.4	sdO	15.7	40 100 ± 600	5.35 ± 0.11	−2.0 ± 0.2	$3.3^{+0.5}_{-0.4}$	3.0098	50.0 ± 11.5	5	*−6.82*
J181126.83+233413.7	sdB	18.4	–	–	–	–	1.0156	121.0 ± 20.5	7	*−6.47*
J204448.63+153638.8[a]	sdB	17.9	29 600 ± 600	5.57 ± 0.09	−2.2 ± 0.1	$5.7^{+0.7}_{-0.7}$	3.0489	101.0 ± 17.5	7	*−6.41*
J185414.11+175200.2	sdOB	16.9	35 200 ± 700	5.89 ± 0.08	−1.4 ± 0.1	$2.9^{+0.3}_{-0.3}$	6.0874	81.0 ± 22.0	10	*−6.25*
J171629.92+575121.2[a]	sdOB	18.2	37 500 ± 800	5.57 ± 0.10	<−0.7	$7.8^{+1.0}_{-0.9}$	3195.9096	67.0 ± 15.5	12	*−6.14*
J184434.74+412158.7	sdB	17.3	27 200 ± 500	5.57 ± 0.12	−2.6 ± 0.1	$4.0^{+0.7}_{-0.6}$	2.9795	56.0 ± 14.0	5	*−5.72*
J091136.73+124015.2	sdB	18.2	–	–	–	–	0.0173	75.0 ± 16.5	3	*−5.31*
J151337.80+195012.5	sdB	18.9	–	–	–	–	0.0354	98.0 ± 33.5	4	*−5.16*
J172727.55+091215.5[i]	sdO	17.5	40 100 ± 1100	5.36 ± 0.09	<−2.1	$7.4^{+0.9}_{-0.8}$	0.0141	55.0 ± 10.5	6	*−5.10*
J112242.69+613758.5[a]	sdB	15.4	29 300 ± 500	5.69 ± 0.10	−2.3 ± 0.3	$1.5^{+0.2}_{-0.2}$	0.0469	83.0 ± 18.5	6	*−5.08*
J161140.50+201857.0[a]	sdOB	18.5	36 900 ± 700	5.89 ± 0.13	−1.2 ± 0.1	$6.1^{+1.1}_{-0.9}$	0.9472	108.0 ± 23.5	5	*−4.77*
J065044.30+383133.7	sdOB	17.3	34 200 ± 400	5.76 ± 0.07	−2.9 ± 0.2	$3.9^{+0.4}_{-0.3}$	0.0131	88.0 ± 13.5	14	*−4.63*
J170645.57+243208.6[a]	sdB	17.8	32 000 ± 500	5.59 ± 0.07	<−4.0	$5.5^{+0.6}_{-0.5}$	0.0125	46.0 ± 12.0	3	*−4.41*
J083359.65-043521.9	sdOB	18.3	36 100 ± 500	5.92 ± 0.11	−1.9 ± 0.2	$5.5^{+0.8}_{-0.7}$	14.9765	88.0 ± 25.5	11	*−4.39*
J140545.25+014419.0[a]	sdB	15.8	27 300 ± 800	5.37 ± 0.16	−1.9 ± 0.2	$2.5^{+0.6}_{-0.5}$	0.0263	25.0 ± 8.0	3	*−4.12*
J160534.96+062733.5	sdB	19.3	–	–	–	–	1.0113	132.0 ± 41.0	8	*−3.97*
J221920.67+394603.5	sdO	17.3	47 000 ± 3500	5.73 ± 0.16	<−3.0	$4.7^{+1.2}_{-0.9}$	62.8679	66.0 ± 12.5	8	*−3.93*
J183840.52+400226.8	sdB	17.8	29 300 ± 900	5.52 ± 0.13	−1.6 ± 0.2	$5.5^{+1.1}_{-0.9}$	2.9795	74.0 ± 20.0	5	*−3.89*
J115716.37+612410.7[a]	sdB	17.2	29 900 ± 500	5.59 ± 0.08	−3.2 ± 0.8	$4.0^{+0.5}_{-0.4}$	2250.6902	102.0 ± 27.0	7	*−3.63*
J113303.70+290223.0[a]	sdB/DA	18.9	–	–	–	–	0.0158	95.0 ± 30.0	3	*−3.39*
J161817.65+120159.6[a]	sdB	18.0	32 100 ± 1000	5.35 ± 0.23	< 0.0	$8.1^{+2.8}_{-2.1}$	0.0427	105.0 ± 28.0	4	*−3.35*
J205101.72+011259.7	sdB+X	17.6	–	–	–	–	0.0141	91.0 ± 31.5	8	*−3.28*
J133638.81+111949.4[a]	sdB	17.3	27 500 ± 500	5.49 ± 0.08	−2.7 ± 0.2	$4.4^{+0.5}_{-0.5}$	0.0301	48.0 ± 14.0	3	*−3.25*
J094044.07+004759.6[h]	sdB	19.1	37 000 ± 800	5.82 ± 0.13	−0.1 ± 0.1	$8.8^{+1.5}_{-1.3}$	2982.7971	30.0 ± 8.5	2	*−3.24*
J210454.89+110645.5[a]	sdOB	17.3	37 800 ± 700	5.63 ± 0.10	−2.4 ± 0.2	$4.9^{+0.6}_{-0.6}$	2548.0064	139.0 ± 27.5	9	*−3.14*
J211651.96+003328.5[a]	sdB	18.0	27 900 ± 800	5.78 ± 0.15	−3.9 ± 0.7	$4.3^{+0.9}_{-0.8}$	0.0161	47.0 ± 15.0	3	*−3.08*
J091428.87+125023.8	sdB	18.0	33 600 ± 600	5.54 ± 0.11	<−3.0	$7.0^{+1.1}_{-0.9}$	0.0176	49.0 ± 13.5	3	*−3.07*

Table 3. Parameters of 18 helium-rich hot subdwarfs (6 RV variable, 12 RV variable candidates).

Name	Class	m_V [mag]	$T_{\rm eff}$ [K]	log g	log y	d [kpc]	Δt [d]	$\Delta \rm RV_{max}$ [km s^{-1}]	N	ln p
J232757.46+483755.2[a]	He-sdO	15.8	64 700 ± 2000	5.40 ± 0.08	>+2.0	$4.2^{+0.5}_{-0.4}$	1799.6136	176.0 ± 20.5	59	−680.31
J141549.05+111213.9[a]	He-sdO	16.1	43 100 ± 800	5.81 ± 0.17	>+2.0	$2.4^{+0.5}_{-0.4}$	0.0075	125.0 ± 17.0	35	−86.42
J103549.68+092551.9[a]	He-sdO	16.3	48 100 ± 600	6.02 ± 0.13	>+2.0	$2.2^{+0.4}_{-0.3}$	3541.9636	53.0 ± 4.0	6	−54.25
J170045.09+391830.3	He-sdOB	18.2	36 500 ± 1600	5.87 ± 0.16	+0.1 ± 0.1	$5.5^{+1.2}_{-1.0}$	2160.0414	118.0 ± 11.5	10	−44.76
J161014.87+045046.6	He-sdO	17.3	48 400 ± 1400	6.31 ± 0.09	>+2.0	$2.5^{+0.3}_{-0.3}$	0.0124	138.0 ± 17.0	14	−31.77
J110215.45+024034.1[a]	He-sdO	17.5	56 600 ± 4200	5.36 ± 0.22	>+2.0	$8.9^{+3.0}_{-2.2}$	0.0332	62.0 ± 8.5	3	−10.91
J174516.32+244348.3[a]	He-sdO	17.7	43 400 ± 1000	5.62 ± 0.21	>+2.0	$6.2^{+1.8}_{-1.4}$	1220.5806	134.0 ± 25.5	13	*−8.81*
J160304.07+165953.8[b]	He-sdO	16.9	45 400 ± 300	6.10 ± 0.07	>+2.0	$2.5^{+0.2}_{-0.2}$	0.9087	71.0 ± 18.5	5	*−8.11*
J094856.95+334151.0[a]	He-sdO	17.7	51 000 ± 1200	5.87 ± 0.12	+1.8 ± 0.5	$5.1^{+0.8}_{-0.7}$	0.0123	74.0 ± 14.0	3	*−7.73*
J152136.25+162150.3	He-sdO	17.1	47 400 ± 1000	5.81 ± 0.08	+1.6 ± 0.4	$4.0^{+0.4}_{-0.4}$	2175.9687	77.0 ± 24.0	9	*−5.94*
J163416.08+221141.0	He-sdOB	15.5	38 300 ± 1400	5.65 ± 0.26	>+2.0	$2.0^{+0.8}_{-0.6}$	653.3309	35.0 ± 6.5	6	*−5.55*
J153237.94+275636.9	He-sdO	18.5	37 700 ± 1300	6.09 ± 0.22	+0.0 ± 0.2	$5.0^{+1.5}_{-1.2}$	1.0012	73.0 ± 16.5	3	*−5.52*
J233914.00+134214.3	He-sdO	17.6	48 100 ± 1600	5.65 ± 0.25	>+2.0	$6.0^{+2.1}_{-1.6}$	1451.6391	72.0 ± 11.8	12	*−5.11*
J173034.09+272139.8[c]	He-sdO	18.9	39 500 ± 700	5.83 ± 0.17	+0.1 ± 0.1	$8.1^{+1.8}_{-1.5}$	698.7112	41.0 ± 10.0	2	*−5.00*
J170214.00+194255.1[b]	He-sdO	15.8	44 300 ± 600	5.79 ± 0.11	>+2.0	$2.1^{+0.3}_{-0.3}$	1665.2088	38.0 ± 10.0	5	*−3.76*
J081329.81+383326.9	He-sdO	17.5	45 800 ± 800	6.11 ± 0.11	+1.8 ± 0.4	$3.3^{+0.5}_{-0.4}$	0.0175	54.0 ± 13.0	6	*−3.35*
J204940.85+165003.6[a]	He-sdO	17.9	43 000 ± 700	5.71 ± 0.13	>+2.0	$6.2^{+1.1}_{-0.9}$	5.9325	84.0 ± 18.5	7	*−3.13*
J160623.21+363005.4	He-sdOB	18.5	36 400 ± 700	5.34 ± 0.17	−0.5 ± 0.1	$11.3^{+2.6}_{-2.1}$	1414.9811	67.0 ± 19.5	2	*−3.04*

Notes. [(a)] Atmospheric parameters taken from Geier et al. (2011a). [(b)] Atmospheric parameters derived from a spectrum taken with ESO-VLT/FORS1. [(c)] Atmospheric parameters derived from a spectrum taken with WHT/ISIS.

Table 4. Parameters of 10 other types of hot stars (5 RV variable, 5 RV variable candidates).

Name	Class	m_V [mag]	$T_{\rm eff}$ [K]	log g	log y	d [kpc]	Δt [d]	$\Delta \rm RV_{max}$ [km s^{-1}]	N	ln p
J131916.15-011404.9	BHB	16.4	17 400 ± 800	4.55 ± 0.15	−1.9 ± 0.2	$5.9^{+1.4}_{-1.1}$	2888.0925	46.0 ± 9.0	8	−42.10
J164121.22+363542.7	BHB	17.4	19 300 ± 1000	4.55 ± 0.10	−1.9 ± 0.2	$9.9^{+1.7}_{-1.4}$	1035.9093	99.0 ± 9.0	8	−39.13
J075732.18+184329.3[a]	O(He)	18.6	80 000 ± 2000	5.00 ± 0.30	>+2.0	$29.6^{+12.7}_{-9.0}$	0.0216	107.0 ± 22.0	6	−30.13
J155610.40+254640.3[b]	PG 1159	17.9	$100\,000^{+15000}_{-10\,000}$	5.3 ± 0.3	>+2.0	$16.9^{+8.9}_{-5.6}$	231.1694	116.0 ± 21.0	10	−17.98
J201302.58-105826.1	MS-B	18.5	16 400 ± 1400	4.30 ± 0.27	−1.3 ± 0.2	$51.8^{+23.6}_{-16.4}$	2.0155	61.0 ± 11.5	8	−13.42
J093521.39+482432.4	O(H)	18.5	87 700 ± 20000	5.68 ± 0.16	−1.0 ± 0.3	$12.0^{+3.7}_{-3.3}$	2269.7542	38.0 ± 7.5	2	*−6.97*
J161253.21+060538.7	MS-B	15.5	15 700 ± 1400	4.18 ± 0.29	−1.0 ± 0.2	$14.4^{+7.2}_{-4.8}$	811.5968	38.0 ± 7.0	10	*−6.84*
J020531.40+134739.8[c]	BHB	18.4	17 400 ± 700	4.26 ± 0.13	−1.7 ± 0.2	$20.3^{+4.0}_{-3.4}$	2781.1087	28.0 ± 7.0	3	*−3.64*
J144023.58+135454.7	BHB	18.3	18 900 ± 700	4.50 ± 0.15	−1.9 ± 0.3	$16.1^{+3.6}_{-3.0}$	0.0528	78.0 ± 24.0	4	*−3.15*
J171947.87+591604.2	MS-B	16.9	15 100 ± 600	4.10 ± 0.19	−0.9 ± 0.2	$29.2^{+8.3}_{-6.5}$	2568.7218	32.0 ± 6.5	10	*−3.11*

Notes. [(a)] Atmospheric parameters taken from Werner et al. (2014). [(b)] Atmospheric parameters taken from Reindl et al. (2016). [(c)] Atmospheric parameters derived from a spectrum taken with ESO-VLT/FORS1.

Table 5. Parameters of 67 stars with non-significant RV variations.

Name	Class	m_V [mag]	$T_{\rm eff}$ [K]	$\log g$	$\log y$	d [kpc]	Δt [d]	$\Delta RV_{\rm max}$ [km s^{-1}]	N	$\ln p$
J112014.86+412127.3	sdB	18.1	–	–	–	–	1503.8023	23.0 ± 7.5	2	−2.98
J173614.19+335249.5	sdB	18.8	–	–	–	–	0.0410	85.0 ± 26.0	5	−2.97
J092520.70+470330.6[a]	sdB	17.7	28 100 ± 900	5.17 ± 0.15	−2.5 ± 0.2	$7.5^{+1.7}_{-1.4}$	0.0126	40.0 ± 12.5	3	−2.88
J171617.33+553446.7[a]	sdB	17.2	32 900 ± 900	5.48 ± 0.09	<−3.0	$4.9^{+0.7}_{-0.6}$	0.0125	130.0 ± 40.5	9	−2.85
J064809.54+380850.1	sdB	18.4	29 300 ± 800	5.26 ± 0.13	−2.8 ± 0.3	$9.8^{+1.9}_{-1.6}$	0.9989	48.0 ± 13.0	5	−2.85
J075937.15+541022.2[a]	sdB	17.8	31 300 ± 700	5.30 ± 0.10	−3.3 ± 0.3	$7.6^{+1.1}_{-1.0}$	0.0233	40.0 ± 18.5	3	−2.75
J001844.33-093855.0	sdB	18.8	–	–	–	–	1169.8455	27.0 ± 8.0	3	−2.75
J112414.45+402637.1[a]	He-sdO	18.0	47 100 ± 1000	5.81 ± 0.23	>+1.7	$5.9^{+1.9}_{-1.4}$	0.0215	62.0 ± 18.5	3	−2.65
J161059.80+053625.2[b]	He-sdO	17.2	46 300 ± 700	6.22 ± 0.10	+1.0 ± 0.6	$2.6^{+0.3}_{-0.3}$	751.7674	38.0 ± 9.5	4	−2.64
J130439.57+312904.8[a]	sdOB	17.1	38 100 ± 600	5.69 ± 0.12	−0.4 ± 0.1	$4.1^{+0.6}_{-0.6}$	0.0163	49.0 ± 27.5	3	−2.63
J143347.59+075416.9	sdOB	16.7	36 600 ± 600	6.16 ± 0.13	<−0.5	$1.9^{+0.3}_{-0.3}$	805.7659	52.0 ± 10.5	11	−2.61
J151415.66-012925.2[a]	He-sdO	17.0	48 200 ± 500	5.85 ± 0.08	+1.7 ± 0.4	$3.6^{+0.4}_{-0.3}$	3.9687	66.0 ± 20.5	5	−2.58
J153540.30+173458.8	sdB	18.0	–	–	–	–	0.0168	58.0 ± 16.5	3	−2.57
J202758.63+773924.5[a]	sdO	17.9	46 200 ± 3200	5.48 ± 0.18	−2.8 ± 0.9	$8.2^{+2.2}_{-1.8}$	1.9601	114.0 ± 33.0	3	−2.48
J215648.71+003620.7[a]	sdB	18.0	30 800 ± 800	5.77 ± 0.12	−2.2 ± 0.3	$4.7^{+0.8}_{-0.7}$	822.1114	100.0 ± 28.0	6	−2.38
J073701.45+225637.6	sdB	16.8	28 100 ± 300	5.45 ± 0.04	<−3.0	$3.7^{+0.2}_{-0.2}$	2.0639	53.0 ± 14.5	5	−2.36
J220810.05+115913.9	sdB	17.4	27 200 ± 600	5.23 ± 0.07	−2.3 ± 0.3	$6.1^{+0.6}_{-0.6}$	2172.7020	42.0 ± 12.5	5	−2.31
J172919.04+072204.5	sdO	17.3	49 200 ± 1900	5.78 ± 0.12	−3.0 ± 0.4	$4.6^{+0.8}_{-0.7}$	0.0179	58.0 ± 20.0	5	−2.22
J100019.98-003413.3	O(H)	17.8	93 700 ± 10700	5.88 ± 0.10	−0.6 ± 0.2	$7.3^{+1.3}_{-1.1}$	3.0114	135.0 ± 28.0	16	−2.20
J031226.01+001018.2	sdB	19.2	–	–	–	–	2552.8670	71.0 ± 30.5	2	−2.17
J204546.81-054355.6[a]	sdB	17.9	35 500 ± 500	5.47 ± 0.09	−1.4 ± 0.2	$7.3^{+0.9}_{-0.8}$	0.0128	41.0 ± 16.5	4	−2.15
J133200.95+673325.7	sdOB	17.2	37 400 ± 500	5.90 ± 0.09	−1.5 ± 0.1	$3.4^{+0.4}_{-0.4}$	2584.9083	53.0 ± 14.5	7	−2.09
J120427.94+172745.3	sdB	18.3	25 100 ± 900	5.25 ± 0.15	−2.6 ± 0.4	$8.2^{+1.9}_{-1.5}$	0.0282	68.0 ± 29.0	3	−2.05
J204550.97+153536.3	sdB	18.2	30 300 ± 500	5.62 ± 0.09	<−3.0	$6.3^{+0.8}_{-0.7}$	5.9148	58.0 ± 13.5	7	−1.98
J135807.96+261215.5[a]	sdB	17.9	33 500 ± 600	5.66 ± 0.10	>+2.0	$5.8^{+0.8}_{-0.7}$	0.0302	86.0 ± 26.0	6	−1.89
J113935.45+614953.9[a]	sdB	16.9	28 800 ± 900	5.27 ± 0.15	−2.8 ± 0.3	$4.9^{+1.1}_{-0.9}$	0.0112	30.0 ± 10.5	3	−1.86
J161938.64+252122.4	He-sdOB	17.5	35 000 ± 2000	5.80 ± 0.33	−0.4 ± 0.2	$4.3^{+2.1}_{-1.5}$	0.9716	67.0 ± 26.0	3	−1.81
J155343.39+131330.4	sdOB	18.5	36 300 ± 500	5.63 ± 0.16	−0.8 ± 0.1	$8.1^{+1.7}_{-1.4}$	0.0160	64.0 ± 24.0	3	−1.77
J110256.32+010012.3[b]	BHB	18.5	17 300 ± 800	4.32 ± 0.14	−2.1 ± 0.2	$19.5^{+4.3}_{-3.5}$	2735.5338	24.0 ± 9.0	3	−1.77
J160450.44+051909.2	He-sdOB	18.5	38 100 ± 700	5.22 ± 0.27	+1.2 ± 0.2	$13.7^{+5.2}_{-3.8}$	0.9736	145.0 ± 61.0	8	−1.75
J082657.29+122818.1	sdOB	17.1	36 500 ± 400	5.83 ± 0.12	−1.4 ± 0.1	$3.4^{+0.5}_{-0.5}$	0.0142	67.0 ± 22.0	4	−1.73
J152705.03+110843.9[a]	sdOB	17.3	37 600 ± 500	5.62 ± 0.10	−0.5 ± 0.1	$4.8^{+0.6}_{-0.5}$	0.0543	43.0 ± 12.0	5	−1.73
J052544.93+630726.0[a]	sdOB	17.7	35 600 ± 800	5.85 ± 0.10	−1.6 ± 0.2	$4.3^{+0.6}_{-0.5}$	0.0264	42.0 ± 15.0	5	−1.73
J100535.76+223952.1[a]	sdB	18.4	29 000 ± 700	5.43 ± 0.13	−2.7 ± 0.2	$7.9^{+1.5}_{-1.3}$	0.0192	41.0 ± 14.0	4	−1.71
J204149.38+003555.8[b]	BHB	19.0	19 400 ± 2200	4.02 ± 0.29	−2.1 ± 0.4	$38.3^{+20.3}_{-13.4}$	38.0700	26.0 ± 10.5	3	−1.71
J164204.37+440303.2	sdB	16.8	29 300 ± 800	5.09 ± 0.13	−2.5 ± 0.3	$5.7^{+1.1}_{-0.9}$	0.0273	31.0 ± 11.5	4	−1.68
J090252.99+073533.9	He-sdO	17.4	40 100 ± 500	5.91 ± 0.19	>+2.0	$3.7^{+0.9}_{-0.7}$	1612.4334	67.0 ± 27.0	5	−1.65
J090957.82+622927.0	sdO	16.4	48 000 ± 4900	5.68 ± 0.17	−1.7 ± 0.6	$3.4^{+1.0}_{-0.8}$	0.0461	37.0 ± 12.0	4	−1.64
J152458.81+181940.5	sdO	18.3	52 300 ± 2500	5.28 ± 0.08	−2.8 ± 0.3	$13.5^{+1.7}_{-1.5}$	0.0155	41.0 ± 15.0	3	−1.60
J112140.20+183613.7	sdB	18.6	28 100 ± 500	5.46 ± 0.10	−1.8 ± 0.1	$8.3^{+1.2}_{-1.0}$	0.9796	71.0 ± 26.0	4	−1.57
J151254.55+150447.0	sdOB	17.8	38 300 ± 600	6.01 ± 0.10	−1.5 ± 0.2	$4.0^{+0.5}_{-0.5}$	0.0229	65.0 ± 28.0	3	−1.54
J233406.11+462249.3[a]	sdB	17.7	34 600 ± 500	5.71 ± 0.09	−1.3 ± 0.1	$4.9^{+0.6}_{-0.6}$	0.0248	31.0 ± 12.0	3	−1.53
J095054.97+460405.2	sdB	18.0	28 500 ± 500	5.24 ± 0.07	−2.3 ± 0.3	$8.1^{+0.8}_{-0.8}$	0.0390	42.0 ± 16.5	3	−1.52
J081304.04-071306.5	He-sdO	18.6	48 200 ± 900	5.93 ± 0.14	+1.8 ± 0.5	$7.0^{+1.3}_{-1.1}$	0.9897	137.0 ± 41.0	7	−1.50
J112526.95+112902.6	sdOB	17.4	36 100 ± 700	6.06 ± 0.12	−0.8 ± 0.1	$2.9^{+0.5}_{-0.4}$	0.0142	70.0 ± 31.0	4	−1.50
J163834.68+265110.2	sdOB	17.0	36 000 ± 300	5.80 ± 0.05	−1.6 ± 0.1	$3.4^{+0.2}_{-0.2}$	0.0159	40.0 ± 13.0	4	−1.50
J203017.81+131849.2	sdOB	16.8	37 100 ± 500	5.92 ± 0.09	−1.4 ± 0.1	$2.7^{+0.3}_{-0.3}$	1200.7860	52.0 ± 20.0	5	−1.47
J130059.20+005711.7[a]	sdOB	16.5	40 700 ± 500	5.53 ± 0.10	−0.6 ± 0.1	$3.9^{+0.5}_{-0.4}$	0.0123	36.0 ± 14.5	3	−1.43
J085727.65+424215.4[a]	He-sdO	18.5	39 500 ± 1900	5.63 ± 0.24	+0.2 ± 0.2	$8.7^{+3.0}_{-2.2}$	0.0657	111.0 ± 39.5	4	−1.26
J074551.13+170600.3	sdOB	17.1	35 600 ± 400	5.54 ± 0.05	−2.8 ± 0.1	$4.7^{+0.3}_{-0.3}$	9.9390	65.0 ± 12.0	18	−1.26
J110445.01+092530.9[a]	sdOB	16.3	35 900 ± 800	5.41 ± 0.07	−2.1 ± 0.4	$3.8^{+0.4}_{-0.3}$	0.0396	34.0 ± 12.0	4	−1.25
J012739.35+404357.8[a]	sdO	16.8	48 300 ± 3200	5.67 ± 0.10	−1.3 ± 0.2	$4.1^{+0.7}_{-0.6}$	0.0369	45.0 ± 17.0	8	−1.23
J172816.87+074839.0	sdB	18.4	30 700 ± 700	5.37 ± 0.09	−2.5 ± 0.4	$9.0^{+1.2}_{-1.1}$	1.9962	75.0 ± 34.0	7	−1.11
J143153.05-002824.3[a]	sdOB	18.1	37 300 ± 800	6.02 ± 0.16	−0.8 ± 0.1	$4.4^{+0.9}_{-0.8}$	0.0120	64.0 ± 20.5	8	−1.05
J225150.80-082612.7[b]	BHB	18.4	19 000 ± 500	4.98 ± 0.09	−1.8 ± 0.3	$9.5^{+1.3}_{-1.1}$	2411.2964	20.0 ± 7.0	5	−1.04
J074806.15+342927.7	sdOB	17.3	35 100 ± 800	5.72 ± 0.08	−1.7 ± 0.1	$4.3^{+0.5}_{-0.5}$	5.9453	42.0 ± 12.5	12	−0.95
J111225.70+392332.7	sdOB	17.6	37 800 ± 500	5.76 ± 0.11	−0.6 ± 0.1	$4.9^{+0.7}_{-0.6}$	0.0563	104.0 ± 28.0	13	−0.92
J134352.14+394008.3[a]	He-sdOB	18.2	36 000 ± 2100	4.78 ± 0.30	−0.2 ± 0.2	$18.8^{+8.5}_{-6.1}$	0.0224	53.0 ± 27.0	3	−0.89
J163702.78-011351.7[a]	He-sdO	17.3	46 100 ± 700	5.92 ± 0.22	>+2.0	$3.8^{+1.1}_{-0.9}$	0.0853	100.0 ± 42.5	12	−0.85
J174442.35+263829.9	sdOB	17.9	–	–	–	–	0.0384	88.0 ± 44.0	7	−0.84
J180757.08+230133.0	He-sdO	17.1	42 700 ± 1000	6.04 ± 0.21	>+2.0	$2.9^{+0.8}_{-0.7}$	0.9992	39.0 ± 19.0	4	−0.83
J204623.12-065926.8	O(H)	17.7	79 500 ± 12500	5.74 ± 0.13	−1.1 ± 0.2	$7.6^{+1.9}_{-1.6}$	1376.1081	47.0 ± 18.0	5	−0.64
J075818.49+102742.5	sdOB	16.4	37 400 ± 600	5.51 ± 0.05	<−3.0	$3.6^{+0.2}_{-0.2}$	0.0596	32.0 ± 12.5	6	−0.57
J215053.84+131650.5	sdB+X	17.0	–	–	–	–	0.0154	24.0 ± 13.5	4	−0.56
J215307.34-071948.3	sdB	17.1	33 100 ± 1300	5.74 ± 0.15	−2.0 ± 0.2	$3.6^{+0.8}_{-0.7}$	24.9831	50.0 ± 27.5	13	−0.42
J113418.00+015322.1[a]	sdB	17.7	29 700 ± 1200	4.83 ± 0.16	<−4.0	$11.8^{+2.9}_{-2.4}$	0.0757	46.0 ± 20.0	6	−0.42
J170716.53+275410.4	sdB	16.7	30 200 ± 1400	5.62 ± 0.16	<−3.0	$3.1^{+0.8}_{-0.6}$	0.0124	52.0 ± 23.0	9	−0.21

Notes. [(a)] Atmospheric parameters taken from Geier et al. (2011a). [(b)] Atmospheric parameters derived from a spectrum taken with ESO-VLT/FORS1.